

Detrended fluctuation analysis of earthquake data

Takumi Kataoka,¹ Tomoshige Miyaguchi,² and Takuma Akimoto^{1,*}

¹*Department of Physics, Tokyo University of Science, Noda, Chiba 278-8510, Japan*

²*Department of Mathematics, Naruto University of Education, Naruto, Tokushima 772-8502, Japan*

(Dated: June 30, 2021)

The detrended fluctuation analysis (DFA) is extensively useful in stochastic processes to unveil the long-term correlation. Here, we apply the DFA to point processes that mimic earthquake data. The point processes are synthesized by a model similar to the Epidemic-Type Aftershock Sequence model, and we apply the DFA to time series $N(t)$ of the point processes, where $N(t)$ is the cumulative number of events up to time t . Crossover phenomena are found in the DFA for these time series, and extensive numerical simulations suggest that the crossover phenomena are signatures of non-stationarity in the time series. We also find that the crossover time represents a characteristic time scale of the non-stationary process embedded in the time series. Therefore, the DFA for point processes is especially useful in extracting information of non-stationary processes when time series are superpositions of stationary and non-stationary signals. Furthermore, we apply the DFA to the cumulative number $N(t)$ of real earthquakes in Japan, and we find a crossover phenomenon similar to that found for the synthesized data.

I. INTRODUCTION

Although stationarity is one of the most important properties in stochastic processes, non-stationary phenomena are rather ubiquitous in nature, ranging from disordered systems [1–6], seismicity [7–10] to biological systems [11–13]. Particularly in point processes, there are two typical types of non-stationary processes. The first (non-stationarity of the first type) is a process in which the probability density function (PDF) for recurrence times depends explicitly on time. Typical examples are rainfalls that exhibit daily and seasonal alterations. The other (non-stationarity of the second type) is a process where a characteristic time scale of the process, such as the mean of the interval between consecutive points, diverges. Owing to divergence, the process never reaches a steady state and thus exhibits non-stationary behaviors [2, 6, 14]. In this study, we focus on non-stationary processes of the first type.

Earthquakes are an example of the non-stationary point process of the first type. One of the most well-known statistical laws of seismicity is the Gutenberg-Richter law [15], which states that the magnitude distribution of earthquakes follows an exponential distribution. This statistical law is universal in the sense that the exponential distributions are observed in any region on earth, any periods and any types of earthquakes such as mainshocks and aftershocks. However, the decay constant, the so-called b -value, depends on time [16]; thus, it is a non-stationary law. Additionally, the Omori law describes a non-stationary property for aftershocks [7], which states that the occurrence rate of aftershocks decays with the time elapsed from the mainshock. More precisely, the occurrence rate decays as a power law: $\lambda(t) \propto t^{-p}$ for large t , where $\lambda(t)$ is the occurrence rate

at elapsed time t after a mainshock, and p (> 0) is a parameter. Since the rate of aftershocks $\lambda(t)$ explicitly depends on t ; aftershocks are intrinsically non-stationary, and earthquake occurrences are non-stationary processes of the first type.

Several methods are proposed to analyze non-stationary time series. For diffusion in heterogeneous environments, trajectories of a diffusing particle can be tracked, and using the trajectory data, the diffusion coefficient can be obtained from the time-averaged mean square displacement (MSD) calculated from the trajectory. If the process is non-stationary, the diffusion coefficient depends explicitly on the total measurement time [6, 11, 12, 17–20]. Thus, plotting the diffusion coefficient as a function of the measurement time provides us information on how the process ages. In another method of non-stationary data analysis of the second type, the inter-occurrence times are utilized frequently [11, 21, 22]. For example, the inter-occurrence-time PDFs have also been extensively used for earthquake researches [23–27].

Although the time-averaged MSD and inter-occurrence-time PDF are useful analysis methods for non-stationary time series of the second type, these methods are not effective in case of the first type. In non-stationary processes of the first type, a long-measurement-time limit of a time average may have a definite value, as the process does not age monotonically. Thus, the diffusion coefficient of time-averaged MSD does not depend on the total measurement time. Moreover, the inter-occurrence-time PDF analysis is based on the fact that the inter-occurrence times are independent and identically distributed (IID). However, this assumption is not valid for nonstationary processes of the first type. Therefore, it is important to develop a method to extract information of nonstationary features from the time series.

In this study, we utilize the detrended fluctuation analysis (DFA), to overcome the above-mentioned difficulties of non-stationary time-series analysis of earthquakes [28].

* takuma@rs.tus.ac.jp

The difference between the DFA and the time-averaged MSD is that the local trends are subtracted in the DFA. The DFA of recurrence times of earthquakes in stationary regimes was studied to unveil the long-term correlation [29]. We note that the DFA can be utilized irrespective of the inter-occurrence times being IID. Here, we apply the DFA to both data synthesized by an earthquake model and data of real earthquakes in non-stationary regimes. In particular, we perform the DFA to a cumulative number $N(t)$ of earthquakes occurred up to time t . As an earthquake model, we employ a simplified version of the Epidemic-Type aftershock sequence model [9].

We find crossover phenomena in DFA for both synthesized and real earthquake data. It is shown that the crossover time represents a characteristic time scale of non-stationary process. Moreover, we present analytical predictions of long time behaviors in DFA for point processes. Until now, relations between the DFA and the long-term correlation in time series have been analytically obtained for fractional Brownian motion (fBm) [30], but it is important to obtain an analytical expression for point processes as well, as these two are totally different stochastic processes [31]. The DFA has been widely used in data analysis, and thus the analytical results for point processes are also useful.

This article is organized as follows. In Sec. II, the earthquake model, which is a superposition of stationary and non-stationary point processes, is proposed, and in Sec. III, the DFA method is briefly reviewed. Sections IV and V present results of DFA for synthesized data and real earthquake data, respectively. Finally, Sec. VI presents a summary and discussion.

II. EARTHQUAKE MODEL

Here, we propose a point process describing occurrences of earthquakes over a vast area, such as the entire extent of Japan. In our model, three types of earthquakes are considered: mainshocks, aftershocks, and stationary earthquakes independent of mainshocks and aftershocks (background earthquakes).

First, we assume that mainshocks occur independently, and thus they are described by a Poisson process. This assumption is quite reasonable because the superposition of large numbers of mutually independent renewal processes becomes a Poisson process in general [32]. In fact, mainshock occurrences have been considered a Poisson process [33, 34]. We have partially confirmed this assumption for a region around Japan by analyzing the Japan Meteorological Agency (JMA) catalog [35], where we define the mainshocks as earthquakes with magnitudes greater than 7. Figure 1 shows that survival probability $P(\tau)$ of inter-occurrence times τ between successive mainshocks follows a superposition of exponential distributions. In the data, the mean inter-occurrence time is around 2.20×10^7 [s] $\cong 254$ [d]. The exponential distribution with mean 2.20×10^7 [s] also well describes the

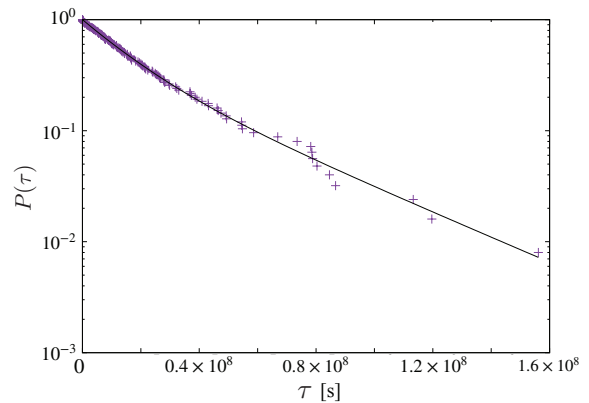


FIG. 1. Survival probability $P(\tau)$ of inter-occurrence times of mainshocks (semi-log plot). There have been 135 mainshocks from January 1, 1923 to April 30, 2017 in Japan. Crosses are a result of real earthquake data. The solid line represents a superposition of the exponential distributions, i.e., $P(\tau) = A \exp(-\lambda_1 \tau) + (1 - A) \exp(-\lambda_2 \tau)$, with $A = 0.59$, $\lambda_1^{-1} \cong 1.48 \times 10^7$ [s] and $\lambda_2^{-1} \cong 3.87 \times 10^7$ [s].

inter-occurrence distribution. Therefore, the mainshock rate λ_m for the entire extent of Japan is approximately given by $\lambda_m \cong 1/2.2 \times 10^{-7}$ [1/s].

Second, we assume that aftershocks are triggered by a mainshock. In particular, we assume that the Omori law [7], which states that the rate of occurrence of aftershocks after a mainshock follows a power-law decay:

$$\lambda_a(t) = \frac{K}{(t+c)^p}, \quad (1)$$

where t is the elapsed time after a mainshock, and K is the degree of the aftershock activity, c is a parameter characterizing the relaxation time of the activity, and p is the power-law exponent. In particular, it has been shown that the parameter p clearly depends on the magnitude of the mainshock [36].

Third, we assume that background earthquakes occur independently of mainshocks and aftershocks. This assumption differs from the Epidemic-Type Aftershock Sequence model [9], where every earthquake is triggered by mainshocks or aftershocks, which are usually triggered by a mainshock. Furthermore, we assume that the rate of the background earthquakes depends on the magnitudes of the mainshocks; that is, when the magnitude of the mainshock is large, the rate of the background earthquakes is also large. It is difficult to determine whether an earthquake is an aftershock or a background earthquake. As we consider earthquakes over a vast region, we assume that almost all earthquakes are independent of mainshocks, and thus are background earthquakes. Under this assumption, we can determine some of the model parameters. Figure 2 shows a schematic view of our model.

A Poisson process with rate λ can be generated by creating inter-event times following the exponential distribution with mean $1/\lambda$ in numerical simulations. In

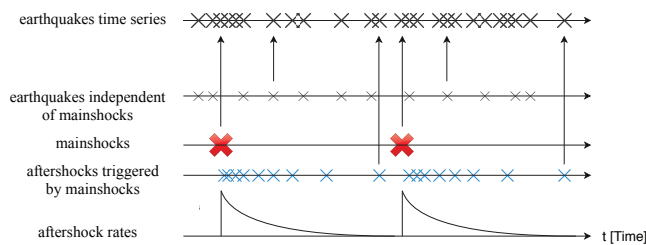


FIG. 2. Schematic view of earthquake model. Earthquake time series are obtained by superposing mainshocks, aftershocks, and background earthquakes. We assume that aftershock rate $\lambda_a(t)$ is the same for each mainshock.

particular, the mainshocks and background earthquakes are generated by Poisson processes with rates λ_s and λ_m , respectively. As aftershocks are described by the Omori's law, we generate them by using a non-stationary Poisson process (see Appendix A for the details). Unlike a non-Markov model of aftershocks [37], it is a Markov model with the exception that it is non-stationary.

III. DETRENDED FLUCTUATION ANALYSIS

The DFA was invented to analyze data that have local trends and non-stationary features [28]. This method has been used to unravel long-range correlations in stationary as well as non-stationary time series such as heartbeat rates, weather variations, recurrence times of earthquakes, and conformation fluctuations of proteins [29, 38–42].

The basic idea is to quantify fluctuations around local trends as

$$F^2(n) \equiv \frac{1}{mn} \sum_{j=0}^{m-1} \sum_{i=jn+1}^{(j+1)n} (y_i - \tilde{y}_i^j)^2, \quad (2)$$

where y_i is a time series that are considered, and \tilde{y}_i^j represents a local trend in the time interval $[jn+1, (j+1)n]$. Thus, n is the length of these time intervals. The local trend \tilde{y}_i^j in the interval $i \in [jn+1, (j+1)n]$ is given by a linear function obtained by the least-square fit to data y_i in the same interval.

Even when there are local trends in data, the function $F(n)$ characterizes a long-term correlation in the data. In particular, $F(n)$ increases as $F(n) \propto n^{1/2}$ when there is no correlation in increments Δy_i of y_i , i.e., $\Delta y_i \equiv y_i - y_{i-1}$. However, it increases as $F(n) \propto n^\alpha$ with $\alpha \neq 1/2$ when the increment has a strong correlation, implying a power-law decay of the correlation function. In particular, $\alpha < 1/2$ implies that there is an anti-correlation in increments Δy_i and $\alpha > 1/2$ implies a positive correlation of increments Δy_i .

Here, we apply the DFA to time series y_i generated by a point process. More precisely, y_i is a monotonically increasing sequence defined by $y_i = N(i)$, where $N(i)$

is the cumulative number of earthquakes up to time i . The variable i is an integer in the original DFA, whereas i in $N(i)$ represents the continuous time; thus, it is a real number. Hence, in what follows, we use t as the argument and use the notation $N(t)$. Note, however, that the definition of the function $F(n)$ in Eq. (2) remains unchanged even for point processes because we only use discrete data points of $N(t)$. In a previous study [43], the DFA for a sequence generated by a point process such as $N(t)$ was studied, where inter-occurrence times are IID random variables. Such a process is called a renewal process. However, the inter-occurrence times may not be IID and the time series are non-stationary of the first type in earthquakes. Here, we investigate the DFA for point processes for such non-stationary time series.

IV. DETRENDED FLUCTUATIONS ANALYSIS ON SYNTHESIZED DATA

In this section, the DFA is applied to three types of data synthesized by the earthquake model: (1) Background earthquakes (Poisson processes), (2) One mainshock and its aftershocks without background earthquakes, and (3) Poissonian mainshocks with aftershocks and background earthquakes. Numerical simulations are carried out for these models and compared with theoretical predictions for small and large n . Derivations of these predictions are presented in Appendices C and D.

A. Background earthquakes (Poisson process)

First, we apply the DFA to Poisson processes, for which inter-occurrence times follow an exponential distribution with rate λ . Figure 3 shows that $F(n)$ increases as $F(n) = An^{1/2}$ for any $n > 0$ and a constant A depends on rate λ of the Poisson process. A theory of the DFA for a Poisson process implies

$$A \cong \sqrt{\frac{\lambda}{15}} \quad (3)$$

(a proof is given in Appendix C), which is confirmed using numerical simulations (inset of Fig. 3). As a Poisson process is a memory-less process, the scaling of $F(n) \propto n^{1/2}$ is quite reasonable. However, we numerically find that scaling $n^{1/2}$ is no longer valid for renewal processes where the PDF of inter-occurrence times follows a power-law distribution with a divergent mean. Therefore, scaling $n^{1/2}$ represents the signature of a stationary Poisson process. In a biased continuous-time random walk, the variance of the displacement, which is a quantity similar to the DFA, shows an anomalous scaling [44, 45].

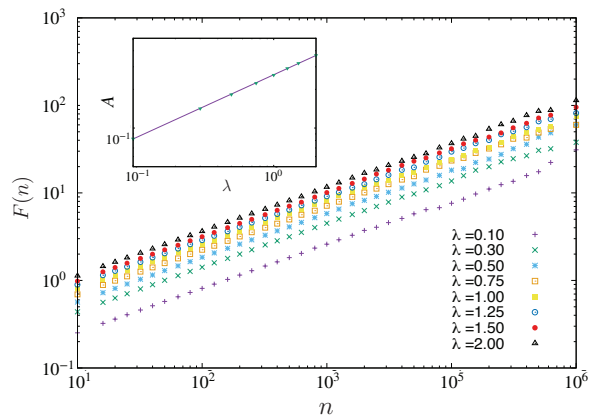


FIG. 3. Detrended fluctuation analysis of $N(t)$ in Poisson processes for different λ , where the total length of the time series is fixed at 10^7 . Inset: constant A as a function of λ . The solid line represents $A = \sqrt{\lambda}/\sqrt{15}$

B. One mainshock and its aftershocks without background earthquakes

Second, synthesized data $N(t)$ are generated using the earthquake model. To obtain a deeper understanding of the features of the DFA, we consider a simple situation where a mainshock occurs only once at $t = 0$, and there are no background earthquakes, i.e., the time series comprises one mainshock and its aftershocks.

As shown in Fig. 4, all the results of the DFA show a crossover from $n^{1/2}$ to n^α scaling. For small- n behavior, $F(n)$ shows $F(n) = Bn^{1/2}$. By an adiabatic approximation, we approximately obtain B :

$$B \cong \frac{\sqrt{\bar{\lambda}_a}}{\sqrt{15}}, \quad (4)$$

where

$$\bar{\lambda}_a = \frac{1}{T} \int_0^T \lambda_a(t) dt \quad (5)$$

and T is the total length of the time series. For large- n behavior, $F(n)$ also shows

$$F(n) \sim \frac{K}{2\sqrt{T}} n^{1/2} \quad (6)$$

when $p = 1$ (see Appendix. D). Equation (6) is a special case of a general result for $p < 3/2$

$$F(n) \sim \frac{Kp}{\sqrt{T(3-2p)(3-p)(2-p)}} n^{3/2-p}, \quad (7)$$

which is valid for $n \rightarrow \infty$ (see Appendix. D). Thus, the power-law exponent in the DFA is determined by p . In other words, the parameter p can be obtained from the asymptotic behavior of the DFA for $N(t)$. This is one of the most important analytical results of our study.

Figure 4 summarizes the results of the DFAs of $N(t)$ for different parameters. Figure 4(a) shows that crossover time n_c in $F(n)$ increases with increasing parameter c and short- n behaviors are almost the same. For large- n behavior, $F(n)$ converges to a $n^{1/2}$ scaling, which does not depend on c . As shown in Figs. 4(b) and (c), crossover time n_c also depends on K and p , but the dependencies are relatively weak compared with the c dependency. Importantly, crossover time n_c is thus almost proportional to c . Therefore, the parameter c can be estimated from the crossover time n_c . This is significantly important when time series are a superposition of non-stationary and stationary signals, because information of the non-stationary part can be obtained without distinguishing the stationary and non-stationary time series. In Fig. 4, it is clearly shown that the asymptotic behaviors of $F(n)$ exhibit different power-law scaling with exponent $3/2-p$. Therefore, the parameter p can be obtained from the asymptotic behavior of the DFA for $N(t)$ if background earthquakes are removed from the time series.

C. Poissonian mainshocks with aftershocks and background earthquakes

For synthesized data $N(t)$ generated by the earthquake model with several mainshocks, we find a crossover phenomenon such that $F(n)$ exhibits a $n^{1/2}$ to n^α scaling. The superposition of two Poisson processes with rates λ_1 and λ_2 is equivalent to a Poisson process with rate $\lambda_1 + \lambda_2$. Therefore, the DFA for the superposition of the two Poisson processes with rates λ_1 and λ_2 becomes $F(n) = \sqrt{(\lambda_1 + \lambda_2)n}/\sqrt{15}$. The synthesized time series are composed of background earthquakes and aftershocks triggered by a mainshock. Since background earthquakes and mainshocks are described by Poisson processes with rates λ_b and λ_m , the above estimation can be utilized. For small- n behavior, $F(n)$ shows that $F(n) \simeq Cn^{1/2}$ and C can be approximately obtained as

$$C \cong \frac{\sqrt{\lambda_b + \lambda_m \times N_a}}{\sqrt{15}}, \quad (8)$$

where

$$N_a = \int_0^{1/\lambda_m} \lambda_a(t) dt. \quad (9)$$

The small- n behavior of the DFA for $N(t)$ is determined by λ_b , λ_m , and N_a .

V. DETRENDED FLUCTUATION ANALYSIS ON EARTHQUAKE DATA CATALOG

Here, we apply the DFA to the cumulative number $N(t)$ of real earthquakes included in the JMA catalog; this catalog contains data of earthquakes with magnitude $M \geq 2$ and the ones that occurred in the area

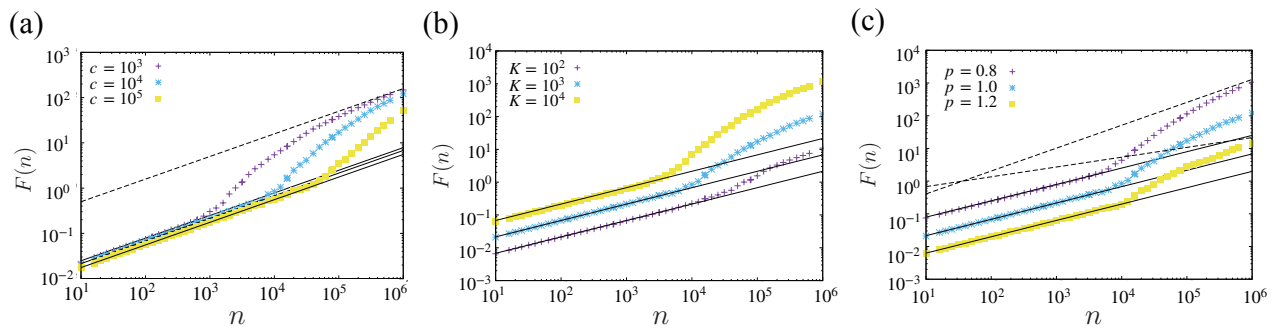


FIG. 4. Detrended fluctuation analysis (DFA) of $N(t)$ for earthquake model, where the length of time series is fixed as 10^7 . (a) DFAs for different values of c . The other parameters are fixed at $p = 1$ and $K = 10^3$. All the solid lines represent $F(n) = Bn^{1/2}$ using Eq. (4). The dashed line represents Eq. (6). (b) DFAs for different K values. The other parameters are fixed at $p = 1$ and $c = 10^4$. (c) DFAs for different values of p . The other parameters are fixed at $c = 10^4$ and $K = 10^3$. All the solid lines represent $F(n) = Bn^{1/2}$ using Eq. (4). The dashed lines represent Eq. (7).

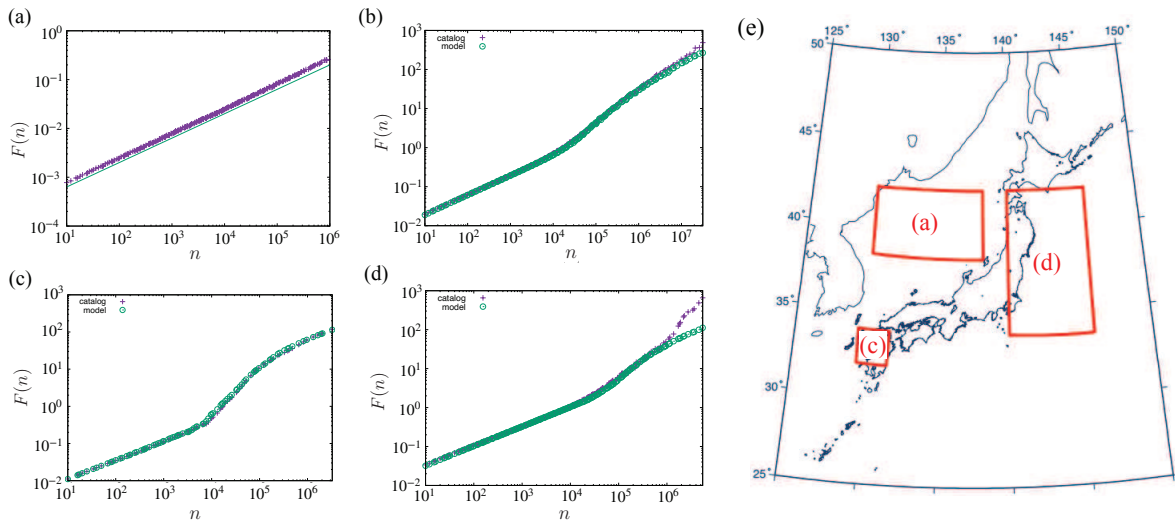


FIG. 5. Detrended fluctuation analysis (DFA) of $N(t)$ for earthquake data. Crosses are the results for the catalog data (real earthquakes), and circles are those for data synthesized with the earthquake models. (a) DFA for time series $N(t)$ with no mainshock at someplace. $N(t)$ is obtained with earthquakes occurred inside the area enclosed within 38° - 42° N latitude and 130° - 138° E longitude [see subplot (e)]. The period of time series $N(t)$ is restricted from January 1, 2009, to December 31, 2010. (b) DFA for time series $N(t)$ with several mainshocks. $N(t)$ is obtained with earthquakes occurred inside the area enclosed within 25° - 50° N latitude and 125° - 150° E longitude. The parameters of the earthquake model are $\lambda_s = 5.0 \times 10^{-4}$, $c = 10^4$, $K = 10^3$, and $p = 1.15$. The period of time series $N(t)$ is restricted from January 1, 2001, to December 31, 2010. (c) DFA for Kumamoto earthquakes. $N(t)$ is obtained with earthquakes occurred inside the area enclosed within 32° - 34° N latitude and 129.5° - 131.5° E longitude [see subplot (e)]. The period of time series $N(t)$ is restricted from April 16, 2016, to April 30, 2017. The parameters of the earthquake model are $\lambda_s = 1.5 \times 10^{-5}$, $c = 10^4$, $K = 5.0 \times 10^3$, and $p = 1.15$. (d) DFA for Tohoku earthquakes. $N(t)$ is obtained with earthquakes occurred inside the area enclosed within 34° - 42° N latitude and 140° - 146° E longitude [see subplot (e)]. The period of time series $N(t)$ is restricted from March 11, 2011, to December 6, 2012. The parameters of the earthquake model are $\lambda_s = 1.5 \times 10^{-3}$, $c = 3.0 \times 10^4$, $K = 10^4$, and $p = 1.2$. (e) Three regions used for the analysis of the subplots (a)(c)(d). The entire region is used for the analysis of the subplot (b).

of 25° - 50° N latitude and 125° - 150° E longitude. Figure 5 shows DFAs for $N(t)$ for several different periods and areas in Japan. We find a crossover phenomenon in $F(n)$; i.e., $F(n)$ increases as $F(n) \propto n^{1/2}$ for small n and $F(n)$ shows another scaling for large n if the data are affected by at least one mainshock. More precisely, $F(n)$

increases as $F(n) \propto n^\alpha$ for $n > n_c$, where $\alpha \cong 1.0$ and $n_c \cong 1.6 \times 10^4$ [s] ($= 4.5$ h). This crossover is observed for all earthquake time series if they contain mainshocks, i.e., earthquakes with magnitudes greater than 7. Moreover, small- n behaviors of $F(n)$ are almost equivalent for all data, while the crossover times n_c are slightly dif-

ferent. Furthermore, we observe that synthesized data $N(t)$ generated by the earthquake model, where parameters are set to be $\lambda_s^{-1} = 2.0 \times 10^3$ [s], $c = 10^4$ [s], $K = 10^3$, and $p = 1.15$, show similar crossover phenomena in the DFA [see Fig. 5(b)]. In this synthesized data, instead of generating mainshocks according to Poisson statistics, mainshocks are assumed to occur at the same times t_i ($i = 1, 2, \dots$) at which real earthquakes with magnitudes greater than 7 occurred.

Furthermore, we applied the DFA to $N(t)$ for specific earthquakes such as the Tohoku and Kumamoto earthquakes. In the Tohoku earthquakes, a mainshock occurred on March 11, 2011, with a magnitude of $M = 9.0$ and we analyzed earthquakes after the mainshock whose area overlaps the area around the epicenter [see Fig. 5(e)]. In the Kumamoto earthquakes, a mainshock occurred on April 16, 2016, with a magnitude of $M = 7.3$, and we analyze earthquakes after the mainshock whose area overlaps the area around the epicenter [see Fig. 5(e)]. In the DFAs for these real earthquakes [Fig. 5(c)(d)], we find crossover phenomena similar to that found for the synthesized data. Moreover, we successfully generate time series $N(t)$ with our earthquake model that reproduce the DFAs of the two earthquake time series, i.e., the Tohoku and Kumamoto earthquakes [circles in Fig. 5(c)(d)]. In the DFA of the Tohoku earthquakes at large n , however, there is a slight difference between the results of the catalog data and the earthquake model. While we assume that a mainshock occurs only at $t = 0$, there are a few mainshocks (earthquakes with magnitudes greater than 7) occurring after $t = 0$ in the catalog data. We believe that such large aftershocks significantly affect subsequent aftershocks. Therefore, our model cannot completely reproduce the DFA of Tohoku earthquakes.

VI. CONCLUSION

We found that crossover phenomena in the DFA of $N(t)$, i.e., the number of earthquakes up to time t , are universally observed in earthquake data. Extensive numerical simulations of the earthquake model show that the crossover phenomena originate from the non-stationarity of the aftershock sequences. In particular, crossover time n_c in the DFA characterizes parameter c , which represents the relaxation time of aftershocks in the Omori's law. Although we do not determine if an earthquake is an aftershock or not, we can successfully obtain information regarding the aftershocks. Therefore, our analysis is significantly important when the time series is a superposition of the two types of time series that cannot be distinguished and when one of the two types is non-stationary and the other is stationary. Moreover, we present theories of the DFA for stationary and non-stationary point processes, which are necessary for performing a thorough analysis.

ACKNOWLEDGEMENT

T.A. was supported by JSPS Grant-in-Aid for Scientific Research (No. C JP18K03468).

Appendix A: Numerical simulations of non-stationary Poisson processes

In numerical simulations of the earthquake model in Sec. II, aftershock sequences, which follow a non-stationary Poisson process, must be generated. Aftershocks triggered by a mainshock are generated as follows: Here, we assume that a mainshock occurs at $t = -t_0$ ($t_0 > 0$). First, time t_0 can be determined as follows: As mainshocks are described by a Poisson process with rate λ_m , t_0 can be obtained by generating a random variable following the exponential distribution with rate λ_m . This is because the random variable t_0 , which is called the backward recurrence time in renewal theory [32], follows the same exponential distribution as the inter-occurrence-time distribution of mainshocks as a result of the memory-less property of Poisson processes [32]. In computer programs, t_0 is obtained by $t_0 = -\lambda_m^{-1} \ln X$, where X is a random variable uniformly distributed on $[0, 1]$.

The probability that an aftershock triggered by the mainshock at $t = -t_0$ occurs at $t = 0$ is given by $\lambda_a(t_0)\Delta t$, where Δt is a time step. In the JMA earthquake catalog, time step Δt is $\Delta t = 1$ [s]. In computer programs, a random variable X is uniformly distributed on $[0, 1]$. Then, we generate an aftershock at $t = 0$ if $X < \lambda_a(t_0)\Delta t$, and no aftershock occurs at $t = 0$ otherwise. This procedure is repeated for $t = \Delta t, 2\Delta t, \dots$ with rates $\lambda_a(t_0 + \Delta t), \lambda_a(t_0 + 2\Delta t), \dots$. In particular, the probability that an aftershock triggered by the mainshock occurs at $t = n\Delta t$ is given by $\lambda_a(t_0 + n\Delta t)\Delta t$.

For simplicity, we generate aftershocks triggered by the mainshock at $t = -t_0$ until the next mainshock occurs at $t = t_1$. This is because the rate of aftershocks triggered by the next mainshock $\lambda_a(t - t_1)$ is much greater than that triggered by the previous mainshock $\lambda_a(t + t_0)$ where $t > t_1$. Similar procedures were employed for the subsequent mainshocks at $t = t_2, t_3, \dots$ and their aftershocks.

Appendix B: Dimensionless form of occurrence rate

Here, we transform the time-dependent occurrence rate $\lambda(t)$ [Eq. (1)] in a dimensionless form. By the following transformation,

$$t \rightarrow t/c \equiv \tilde{t}, \quad \lambda_a(t) \rightarrow c\lambda_a(t) \equiv \tilde{\lambda}_a(\tilde{t}), \quad K \rightarrow c^{1-p}K \equiv \tilde{K}, \quad (\text{B1})$$

we have a non-dimensional occurrence rate

$$\tilde{\lambda}_a(\tilde{t}) = \frac{\tilde{K}}{(\tilde{t} + 1)^p}. \quad (\text{B2})$$

In addition, if the measurement time T is transformed as $T \rightarrow T/c \equiv \tilde{T}$, the remaining parameters are \tilde{K} , \tilde{T} and p .

Appendix C: Theory of DFA for point process

In this study, our objective is the extraction of non-stationary information from point processes using DFA. Here, we provide a theoretical argument regarding the DFA for stationary point processes with constant rate λ .

1. Inter-occurrence-time distribution

We assume that inter-occurrence-time distribution of successive renewals follows a distribution $\psi(\tau)$ with finite mean and variance $\langle \tau \rangle$ and $\langle \tau^2 \rangle - \langle \tau \rangle^2$. For this inter-occurrence-time distribution, the mean and variance of $N(i)$ are given by [32, 46]

$$\langle N(i) \rangle \sim \frac{i}{\langle \tau \rangle}, \quad (\text{C1})$$

$$\langle N^2(i) \rangle - \langle N(i) \rangle^2 \sim \frac{\langle \tau^2 \rangle - \langle \tau \rangle^2}{\langle \tau \rangle^3} i, \quad (\text{C2})$$

In particular, mean interval $\langle \tau \rangle$ is related with the rate λ as $\langle \tau \rangle = 1/\lambda$; thus, Eq. (C1) is rewritten as $\langle N(i) \rangle \sim \lambda i$. For Eq. (C2), we also use a notation $\langle N^2(i) \rangle - \langle N(i) \rangle^2 = \sigma^2 i$, where σ^2 is defined by $\sigma^2 = (\langle \tau^2 \rangle - \langle \tau \rangle^2) / \langle \tau \rangle^3$.

If $\psi(\tau)$ is given by the exponential distribution

$$\psi(\tau) = \frac{1}{\langle \tau \rangle} e^{-\tau/\langle \tau \rangle}, \quad (\text{C3})$$

the point process is referred to as the Poisson process. For the Poisson process Eqs. (C1) and (C2) is given by

$$\langle N(i) \rangle = \frac{i}{\langle \tau \rangle}, \quad (\text{C4})$$

$$\langle N^2(i) \rangle - \langle N(i) \rangle^2 = \frac{i}{\langle \tau \rangle}. \quad (\text{C5})$$

Note that equalities hold for the Poisson process. From the definition of σ^2 , it follows that $\sigma^2 = \lambda$ holds for the Poisson process.

2. Theory of DFA for point process

Based on the stationarity of the point process, Eq. (2) can be represented as

$$F^2(n) = \left\langle \frac{1}{n} \sum_{i=1}^n (y_i - \tilde{y}_i^0)^2 \right\rangle, \quad (\text{C6})$$

where $y_i = N(i)$ is obtained using the point process described above. We rewrite the DFA as

$$F^2(n) = \frac{1}{n} \sum_{i=1}^n \langle [y_i - \lambda i - (\tilde{y}_i^0 - \lambda i)]^2 \rangle \quad (\text{C7})$$

$$= \frac{1}{n} \sum_{i=1}^n [\tilde{y}_i - (ai + b)]^2, \quad (\text{C8})$$

where \tilde{y} is defined as $\tilde{y}_i = y_i - \lambda i$. Moreover, a and b are the coefficients of the linear fitting of \tilde{y}_i by the least-square method, i.e., $\tilde{y}_i^0 - \lambda i = ai + b$. By expanding the summand, we obtain

$$F^2(n) = \frac{1}{n} \sum_{i=1}^n (\langle \tilde{y}_i^2 \rangle - 2i \langle a \tilde{y}_i \rangle - 2 \langle b \tilde{y}_i \rangle + i^2 \langle a^2 \rangle + 2i \langle ab \rangle + \langle b^2 \rangle). \quad (\text{C9})$$

The parameters a and b are given by

$$a = \frac{S_{xy}}{S_x^2} - \lambda, \quad b = \frac{1}{n} - \frac{n+1}{2} \frac{S_{xy}}{S_x^2}, \quad (\text{C10})$$

where S_{xy} and S_x^2 are a covariance and a variance given by

$$S_{xy} = \frac{1}{n} \sum_{j=1}^n j y_j - \frac{1}{n^2} \sum_{j=1}^n j \sum_{k=1}^n y_k, \quad (\text{C11})$$

$$S_x^2 = \frac{1}{n} \sum_{j=1}^n j^2 - \frac{1}{n^2} \left(\sum_{j=1}^n j \right)^2. \quad (\text{C12})$$

It follows that a and b are written as

$$a = \frac{1}{n S_x^2} \sum_{j=1}^n \left(j - \frac{n+1}{2} \right) \tilde{y}_j \quad (\text{C13})$$

$$b = \frac{1}{n} \sum_{j=1}^n \tilde{y}_j - \frac{n+1}{2} a. \quad (\text{C14})$$

In Poisson processes, we have $\langle N(i)N(i+i') \rangle = \langle N^2(i) \rangle + \langle N(i)[N(i') - N(i)] \rangle = \langle N^2(i) \rangle + \langle N(i) \rangle \langle N(i') - N(i) \rangle$, because a Poisson process is a memory-less process, i.e., $N(i)$ and $N(i') - N(i)$ are independent. It follows that $\langle \tilde{y}_i \rangle = 0$, $\langle \tilde{y}_i^2 \rangle = \sigma^2 i$, and $\langle \tilde{y}_i \tilde{y}_j \rangle = \sigma^2 \min(i, j)$. For general point processes, $N(i)$ and $N(i') - N(i)$ are not independent. It becomes

$$\langle \tilde{y}_i \tilde{y}_j \rangle \approx \frac{i+j}{2} \sigma^2 - \frac{|i-j|}{2} \lambda. \quad (\text{C15})$$

By using Eqs. (C13) and (C15), we obtain

$$\sum_{i=1}^n \left(i - \frac{n+1}{2} \right) \langle \tilde{y}_i a \rangle \approx \frac{-\lambda}{nS_x^2} \sum_{i,j=1}^n \left(i - \frac{n+1}{2} \right) \left(j - \frac{n+1}{2} \right) \frac{|i-j|}{2}, \quad (\text{C16})$$

and

$$\langle a^2 \rangle = \frac{-\lambda}{(nS_x^2)^2} \sum_{i,j=1}^n \left(i - \frac{n+1}{2} \right) \left(j - \frac{n+1}{2} \right) \frac{|i-j|}{2}, \quad (\text{C17})$$

where the term $(i+j)\sigma^2/2$ in Eq. (C15) vanishes considering the summation over i and j , because $\sum_{i=1}^n [i - (n+1)/2] = 0$. By Eqs. (C15)–(C17), it follows that the DFA in Eq. (C9) is rewritten as

$$F^2(n) = \frac{1}{n} \sum_{i=1}^n \sigma^2 i - \frac{2}{n} \left[\sum_{i=1}^n \left(i - \frac{n+1}{2} \right) \langle a \tilde{y}_i \rangle + \frac{1}{n} \sum_{i,j=1}^n \langle \tilde{y}_i \tilde{y}_j \rangle \right] \quad (\text{C18})$$

$$+ \frac{1}{n} \sum_{i=1}^n \left[\left(i - \frac{n+1}{2} \right)^2 \langle a^2 \rangle + \frac{2}{n} \sum_{j=1}^n \left(i - \frac{n+1}{2} \right) \langle a \tilde{y}_j \rangle + \frac{1}{n^2} \sum_{j,k=1}^n \langle \tilde{y}_j \tilde{y}_k \rangle \right] \quad (\text{C19})$$

$$\simeq \frac{\sigma^2 n}{2} + \frac{\lambda}{n^2 S_x^2} \sum_{j,k=1}^n \left(j - \frac{n+1}{2} \right) \left(k - \frac{n+1}{2} \right) \frac{|k-j|}{2} - \frac{\sigma^2 n}{2} + \frac{n}{6} \lambda \quad (\text{C20})$$

$$\simeq \frac{\lambda n}{15}, \quad (\text{C21})$$

where we used an approximation, $\sum_{j=1}^n j^k \simeq n^{k+1}/(k+1)$ for $n \rightarrow \infty$. Equation (C18) is valid for any point process that has a finite mean and variance. Thus, Eq. (C18) holds for the Poisson processes, and thus we obtain Eq. (3).

Appendix D: Asymptotic behavior of the DFA for aftershock sequences

Here, we evaluate the asymptotic behavior of the DFA for aftershock sequences in the large- n limit. The mean number of aftershocks is given by $\langle N(t) \rangle = \int_0^t \lambda_a(t') dt'$. Because the derivative of $\langle N(t) \rangle$ tends to zero for $t \rightarrow \infty$, deviations from a linear fitting become zero for the large- t limit. In other words, the deviation in the first time window in $F(n)$ is significant in the large- n limit. Therefore, in the large- n limit, $F(n)$ can be approximately obtained from the first time window:

$$F(n)^2 \simeq \chi_0(n)^2 \equiv \frac{1}{mn} \sum_{i=1}^n (y_i - \tilde{y}_i^0)^2. \quad (\text{D1})$$

In the following, we replace y_i with $\langle N(t) \rangle$ to calculate $\chi_0(n)^2$. Using the least mean square method, we have a linear function, i.e., $\tilde{y}_i^0 \equiv ai + b$.

For $p = 1$, $\langle N(t) \rangle$ is given by

$$\langle N(t) \rangle = K \log \left(\frac{t}{c} + 1 \right). \quad (\text{D2})$$

Using $\partial \chi_0(n)^2 / \partial a = \partial \chi_0(n)^2 / \partial b = 0$, we obtain

$$a = \frac{3K}{n}, \quad b = K \left[\log \left(\frac{n}{c} + 1 \right) - \frac{5}{2} \right]. \quad (\text{D3})$$

We approximate the sum in Eq.(D1) by the integral:

$$\chi_0(n)^2 \simeq \frac{1}{T} \int_0^n \left[K \log \left(\frac{t+c}{n+c} \right) - \frac{3K}{n} t - \frac{5K}{2} \right]^2. \quad (\text{D4})$$

For $n \gg c$, we have

$$F(n) \simeq \frac{K}{2} \sqrt{\frac{n}{T}}. \quad (\text{D5})$$

For $p \neq 1$, $\langle N(t) \rangle$ is given by

$$\langle N(t) \rangle = \frac{c^{1-p} K}{1-p} \left[\left(\frac{t}{c} + 1 \right)^{1-p} - 1 \right]. \quad (\text{D6})$$

In the long- t limit, $\langle N(t) \rangle$ becomes

$$\langle N(t) \rangle \sim \frac{K}{1-p} t^{1-p} \quad (\text{D7})$$

and

$$\langle N(t) \rangle - \frac{c^{1-p} K}{p-1} \sim -\frac{K}{p-1} t^{1-p} \quad (\text{D8})$$

for $p < 1$ and $p > 1$, respectively. In the same calculation as the above, we have

$$F(n) \simeq \frac{Kp}{\sqrt{T(3-2p)(3-p)(2-p)}} n^{\frac{3}{2}-p} \quad (\text{D9})$$

for $p < 3/2$ ($p \neq 1$).

-
- [1] H. Scher and E. W. Montroll, Phys. Rev. B **12**, 2455 (1975).
- [2] J.-P. Bouchaud and A. Georges, Phys. Rep. **195**, 127 (1990).
- [3] J.-P. Bouchaud, J. Phys. I **2**, 1705 (1992).
- [4] C. Monthus and J.-P. Bouchaud, J. Phys. A **29**, 3847 (1996).
- [5] X. Brokmann and *et al.*, Phys. Rev. Lett. **90**, 120601 (2003).
- [6] R. Metzler, J.-H. Jeon, A. G. Cherstvy, and E. Barkai, Phys. Chem. Chem. Phys. **16**, 24128 (2014).
- [7] F. Omori, J. College Sci. Imp. Univ. Tokyo **7**, 111 (1894).
- [8] T. Utsu, J. Facul. Sci. Hokkaido Univ. Ser. VII **3**, 379 (1970).
- [9] Y. Ogata, J. Am. Stat. Assoc. **83**, 9 (1988).
- [10] T. Utsu, *A review of seismicity (in Japanese)*, in *Mathematical Seismology*, edited by M. Saito, Vol. 2 (Inst. of Stat. Math., Tokyo, 1992).
- [11] A. Weigel, B. Simon, M. Tamkun, and D. Krapf, Proc. Natl. Acad. Sci. USA **108**, 6438 (2011).
- [12] E. Yamamoto, T. Akimoto, M. Yasui, and K. Yasuoka, Sci. Rep. **4**, 4720 (2014).
- [13] C. Manzo, J. A. Torreno-Pina, P. Massignan, G. J. Lapeyre Jr, M. Lewenstein, and M. F. G. Parajo, Phys. Rev. X **5**, 011021 (2015).
- [14] T. Akimoto, E. Barkai, and G. Radons, Phys. Rev. E **101**, 052112 (2020).
- [15] B. Gutenberg and C. F. Richter, Bull. Seismol. Soc. Am. **34**, 185 (1944).
- [16] K. Nanjo, N. Hirata, K. Obara, and K. Kasahara, Geophys. Res. Lett. **39** (2012).
- [17] Y. He, S. Burov, R. Metzler, and E. Barkai, Phys. Rev. Lett. **101**, 058101 (2008).
- [18] T. Miyaguchi and T. Akimoto, Phys. Rev. E **83**, 031926 (2011).
- [19] T. Miyaguchi and T. Akimoto, Phys. Rev. E **91**, 010102 (2015).
- [20] T. Akimoto and E. Yamamoto, J. Stat. Mech. **2016**, 123201 (2016).
- [21] I. Y. Wong, M. L. Gardel, D. R. Reichman, E. R. Weeks, M. T. Valentine, A. R. Bausch, and D. A. Weitz, Phys. Rev. Lett. **92**, 178101 (2004).
- [22] M. Kuno, D. P. Fromm, H. F. Hamann, A. Gallagher, and D. J. Nesbitt, J. Chem. Phys. **112**, 3117 (2000).
- [23] A. Corral, Phys. Rev. Lett. **92**, 108501 (2004).
- [24] S. Abe and N. Suzuki, Physica A **350**, 588 (2005).
- [25] A. Saichev and D. Sornette, Phys. Rev. Lett. **97**, 078501 (2006).
- [26] T. Hasumi, T. Akimoto, and Y. Aizawa, Physica A **388**, 491 (2009).
- [27] H. Tanaka and Y. Aizawa, J. Phys. Soc. Jpn **86**, 024004 (2017).
- [28] C.-K. Peng, S. V. Buldyrev, S. Havlin, M. Simons, H. E. Stanley, and A. L. Goldberger, Phys. Rev. E **49**, 1685 (1994).
- [29] S. Lennartz, V. Livina, A. Bunde, and S. Havlin, Europhys. Lett. **81**, 69001 (2008).
- [30] M. S. Taqqu, V. Teverovsky, and W. Willinger, Fractals **03**, 785 (1995).
- [31] M. Magdziarz, A. Weron, K. Burnecki, and J. Klafter, Phys. Rev. Lett. **103**, 180602 (2009).
- [32] D. R. Cox, *Renewal theory* (Methuen, London, 1962).
- [33] J. Gardner and L. Knopoff, Bull. Seismol. Soc. Am. **64**, 1363 (1974).
- [34] Y. Y. Kagan and D. D. Jackson, Geophys. J. Int. **104**, 117 (1991).
- [35] Japan Meteorological Agency Earthquake Catalog, <http://evrrss.eri.u-tokyo.ac.jp/tseis/jma1/index.html>.
- [36] G. Ouillon and D. Sornette, J. Geophys. Res. **110** (2005).
- [37] T. Akimoto and Y. Aizawa, Prog. Theor. Phys. **114**, 737 (2005).
- [38] C.-K. Peng, J. Mietus, J. M. Hausdorff, S. Havlin, H. E. Stanley, and A. L. Goldberger, Phys. Rev. Lett. **70**, 1343 (1993).
- [39] E. Koscielny-Bunde, A. Bunde, S. Havlin, H. E. Roman, Y. Goldreich, and H.-J. Schellnhuber, Phys. Rev. Lett. **81**, 729 (1998).
- [40] S. Havlin, S. Buldyrev, A. Bunde, A. Goldberger, P. C. Ivanov, C.-K. Peng, and H. E. Stanley, Physica A **273**, 46 (1999).
- [41] T. Harada, T. Yokogawa, T. Miyaguchi, and H. Kori, Biophys. J. **96**, 255 (2009).
- [42] E. Yamamoto, T. Akimoto, Y. Hirano, M. Yasui, and K. Yasuoka, Phys. Rev. E **89**, 022718 (2014).
- [43] P. Paradisi, R. Cesari, A. Donato, D. Contini, and P. Allegrini, Nonlinear Proc. Geophys. **19**, 113 (2012).
- [44] T. Akimoto, A. G. Cherstvy, and R. Metzler, Phys. Rev. E **98**, 022105 (2018).
- [45] R. Hou, A. G. Cherstvy, R. Metzler, and T. Akimoto, Phys. Chem. Chem. Phys. **20**, 20827 (2018).
- [46] C. Godrèche and J. M. Luck, J. Stat. Phys. **104**, 489 (2001).